

Development of small cyclic peptides targeting the CK2 α / β interface

Eleanor L. Atkinson,^a Jessica Iegre,^a Claudio D'Amore,^b Paul D. Brear,^c Mauro Salvi,^{*b} Marko Hyvönen^{*c} and David R. Spring.^{*a}

a. Yusuf Hamied Department of Chemistry, University of Cambridge, Lensfield Road, CB2 1EW, Cambridge, UK. Email: spring@ch.cam.ac.uk.

b. Department of Biomedical Sciences, University of Padova, Padova, Italy. Email: mauro.salvi@unipd.it.

c. Department of Biochemistry, University of Cambridge, Tennis Court Road, CB2 1GA, Cambridge, UK. Email: mh256@cam.ac.uk.

Abstract

CK2 is a ubiquitous protein kinase, with key roles in the regulation of cell growth and proliferation. In particular, CK2 acts as an anti-apoptotic protein and is found to be overexpressed in multiple cancer types. To this end, the inhibition of CK2 is of great interest with regard to the development of novel anti-cancer therapeutics. ATP-site inhibition of CK2 is possible; however, this typically results in poor selectivity due to the highly conserved nature of the catalytic site amongst kinases. An alternative methodology for the modulation of CK2 activity is to inhibit the formation of the holoenzyme complex. This is possible, with the most notable example being CAM7117. However, CAM7117 contains unnatural amino acids, residues not directly involved in the binding to CK2, and its size limits further optimisations. In this work, an iterative cycle of enzymatic assays, X-ray crystallography, molecular modelling and cellular assays were used to develop a functionalisable chemical probe for the CK2 α / β PPI. The lead peptide, P8C9, successfully binds to CK2 α at the protein-protein interaction site, is easily synthesisable and functionalisable, highly stable in serum and small enough to accommodate further optimisation. Furthermore, its cell-permeable analogues, TAT-P8C9 and R3-P8C9, successfully inhibit cell proliferation. TAT-P8C9 and R3-P8C9 can serve as true chemical probes to further understand the intracellular pathways involving CK2, as well as aiding the development of novel CK2 PPI inhibitors for therapeutic use.

Introduction

CK2 is a ubiquitous and constitutively active protein kinase.¹ It has a heterotetrameric quaternary structure, consisting of two catalytic subunits (α or α') and two regulatory subunits (β).² The α/α' subunits carry out the phosphorylation of target proteins and peptide substrates, whereas the β subunits confer stability to the enzyme, control substrate specificity, and govern cellular localisation of the holoenzyme complex.³ In particular, CK2 β enhances the catalytic activity of CK2 α , as well as increasing its thermostability.⁴ CK2 β is also necessary for the protein shuttling of CK2 between intracellular compartments and, consequently, it controls the cellular location of the enzyme. Removal of CK2 β from the catalytic subunit prevents the formation of the holoenzyme, resulting in adverse effects upon substrate recognition, the stability of CK2 α , and its intracellular protein shuttling, all altering CK2's effect on the cell cycle.⁵

CK2 acts as an anti-apoptotic protein and is seen to be overexpressed in a wide variety of cancerous tumours.^{3,6-8} The absence of alternative pathways to compensate for CK2 downregulation makes cancer cells particularly sensitive to CK2 inhibition.⁹⁻¹¹ Promisingly, a first-in-class small molecule inhibitor, CX4945, has been designated as an orphan drug by FDA for the treatment of

cholangiocarcinoma, and several clinical studies are ongoing for the treatment of different types of tumours with this molecule, both alone and in combination therapies.¹²

There are multiple ways in which CK2 can be inhibited and the most widely researched of these methods is to target the ATP-binding site, which can be done with the aforementioned inhibitor CX4945.³ More recently, however, there has been a move towards targeting alternative sites on the protein.^{13–15} One such alternative method is *via* the inhibition of the protein-protein interaction (PPI) between the α and β subunits of CK2; the PPI interface is not as well conserved among other kinases as the ATP active site hence its inhibition is considered a more specific approach.² Preventing the formation of the CK2 holoenzyme would induce apoptosis by adjusting the substrate specificity and cellular location of the subunits, thus altering the intracellular environment.¹⁶

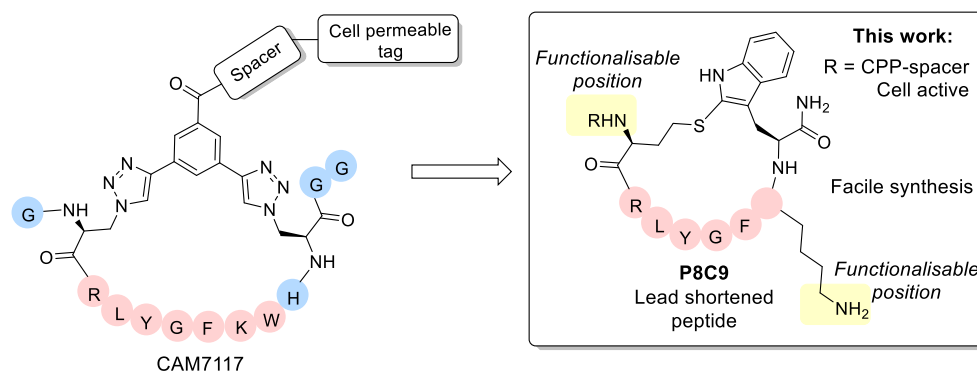
Peptides are good PPI modulators as their flexibility and size allows them to adapt to the large and shallow surfaces involved.¹⁷ This strategy has been applied to target CK2, and a handful of cyclic peptides are known to inhibit the CK2 PPI, most notably Pc, TAT-Pc and CAM7117.^{16,18,19} The most potent inhibitor, CAM7117, shows an improved K_d relative to Pc (200 nM vs 1 μ M respectively), greater stability in human serum and antiproliferative activity in cancer cells.¹⁶ However, the synthesis of CAM7117 requires the use of an expensive unnatural amino acid, a non-commercially available staple, and three purification steps; thus the synthesis is expensive, slow and low yielding.¹⁶ Despite currently being the most potent peptide PPI inhibitor of CK2, its reduced activity in cellular assays and complex synthesis indicates that further work is required to develop a potent and selective peptide which inhibits CK2 in cells and is facilely obtained.

We are building here on the CAM7117 work, developing novel conformationally-constrained peptides which are easily synthesised and with improved physicochemical properties to yield an enhanced chemical probe for the CK2 PPI.

Following iterative cycles of design, synthesis and testing, the sequence of CAM7117 was shortened. A lead sequence, able to bind to CK2 α and simultaneously present the side chains of two amino acids in a suitable position for constraining, was identified before being cyclised using a variety of constraints to obtain a peptide locked in its binding conformation (Fig 1). The binding mode of the lead cyclic peptide was investigated using X-ray crystallography of the ligand in complex with CK2 α . This peptide was then tested in cellular assays to evaluate its ability to reduce cell viability.

Retention of good binding affinity, combined with a reduction in the molecular weight, resulted in an increase in the ligand efficiency of the peptide, whilst addition of a cell penetrating tag provided good cellular activity, with all peptides being facile to synthesise in two steps without needing synthetic staples and complex unnatural amino acids.

Figure 1. Overview of the lead peptides developed in this work compared to the CK2 PPI inhibitor CAM7117.¹⁶ The shortened peptide **P8C9** is easily synthesisable, active in enzymatic assays and functionalisation with a cell penetrating peptide (CPP)-spacer yields good cellular activity. Blue spheres = residues removed from CAM7117 in **P8C9**.



Results and Discussion

Rational design of short CK2 β -like peptides

Analysis of the X-ray crystal structure of unfunctionalised CAM7117 (sequence GX_{C1}RLYGFKWHX_{C1}GG) bound to CK2 α (PDB: 6Q4Q) strongly suggests that the key binding interactions between the peptide and CK2 α are focused within the cyclic portions of the peptide.¹⁶ Therefore, shortened peptides using the central binding sequence of CAM7117 (RLYGFKWH) were chosen to investigate which residues could be used for cyclising the peptide into its binding conformation.

Molecular modelling suggested that only two positions (other than those used in CAM7117) could be used for constraining the central peptide sequence, RLYGFKWH: Trp and Aza-alanine (Aza) residues (ESI Fig S1). Cyclisation of the Trp and Aza residues would allow for even greater shortening of the peptide sequence than simple removal of the terminal Gly residues. Additionally, the distance between the α -carbons of the Trp and Aza residues (7.5 Å) is shorter than between the two Aza residues in CAM7117 (11.6 Å) meaning that the size of the constraint used could also be reduced (ESI Fig S1).

Before proceeding to the synthesis of constrained peptides, a series of linear peptides was synthesised based upon the central sequence of CAM7117 (RLYGFKWH) to determine which amino acids could be removed without compromising activity.

Linear peptide synthesis and analysis

The peptide sequences initially synthesised are outlined in Table 1 alongside that of unfunctionalised CAM7117 (**P₊**, CAM7117 without the tri-Arg tag and spacer). Additionally, a reverse-sequence peptide, **P₋** (HWKFGYLR), was synthesised for use as a negative control in subsequent assays.

To assess the ability of the synthesised linear peptides to displace a CK2 β -like fluorescent probe from CK2 α , a fluorescence polarisation (FP) assay was used (Table 1, ESI 1.3.2 and ESI Fig S2). Comparison of the linear peptides indicates a large drop off in binding with the removal of the Arg (**P2 versus P3**) and Trp residues (**P1 versus P3**), suggesting that they both contribute positively to the activity of the peptide, with the removal of Trp resulting in a more profound loss of activity. The Ile to Trp mutation in CAM7117 resulted in a boost in potency ($K_d = 150$ nM, $K_d = 460$ nM for **P₊** and the corresponding peptide bearing Ile instead of Trp).¹⁶ Therefore, it is unsurprising that removal of the Trp residue resulted in a large loss in activity. Conversely, the His does not appear to be crucial to the binding ability of the peptide and, therefore, it was removed in the design of cyclic peptides.

Table 1 Linear peptide sequences synthesised and the number of residues they contain. All peptides feature an amide at the C-terminus and are acetyl-capped at the N-terminus. X = Aza-alanine. X_{C1} = unfunctionalised constraint in CAM7117.

Peptide	Sequence	No. of residues	IC ₅₀ (μ M)
P1	RLYGFK	6	>500
P2	LYGFKW	6	136.9 \pm 25.8
P3	RLYGFKW	7	22.5 \pm 2.4
P4	RLYGFKWH	8	16.7 \pm 2.3
P₊	GX _{C1} RLYGFKWHX _{C1} GG	13	8.7 \pm 4.2

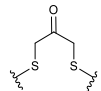
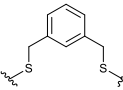
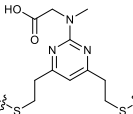
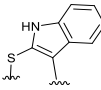
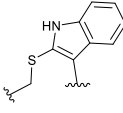
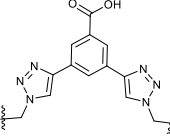
Design and enzymatic evaluation of cyclic peptides

Combining the results of the molecular modelling, crystal structures and the FP of the linear peptides, the design of cyclic peptides was based upon the shortened peptide sequence RLYGFK, with two flanking residues for cyclisation at either end. Although the removal of Trp led to a loss in activity of the linear peptide, it was envisaged that its binding contribution could be compensated for by utilising

an aromatic or hydrophobic staple, mimicking the properties of the Trp residue. For this purpose, the linear sequences CRLYGFKC (**P5**) and JRLYGFKX (**P6**) were used (J = propargylglycine, X = Aza-alanine) with a variety of constraints. Additionally, we considered keeping the Trp residue and stapling with Cys and homoCys (hC) residues using the linear sequences CRLYGKW (**P7**) and (hC)RLYGKW (**P8**) respectively with mild oxidative cyclisation conditions.²⁰ Furthermore, due to the small distance between the cyclising residues (7.9 Å), large constraints such as long alkyl chains and extended aromatic ring structures were ruled out. Instead, relatively small constraints were trialled (ESI Table S1).

Compared to **P+**, **P8C9** showed a greater than 5 times increase in activity in our preliminary assay (ESI Fig S3 and S4), indicating that **P8C9** can efficiently engage CK2α despite its reduced size. A comparison of the LEs of the novel peptides with that of **P+** indicates that **P8C9** uses its structural features to target CK2α the most effectively with a LE of 0.101 vs 0.057 for **P+** (Table 2).

Table 2 Structure of the active cyclic peptides tested, alongside their IC₅₀'s and ligand efficiencies. IC₅₀'s are reported ± SEM. Peptide sequences: **P5CX** = C_{CX}RLYGFKC_{CX}, **P7C8** = C_{C8}RLYGFKW_{C8}, **P8C9** = (hC)_{C9}RLYGFKW_{C9}, **P+** = GX_{C1}RLYGFKWHX_{C1}GG

Peptide	Constraint	IC ₅₀ (μM)	Ligand efficiency
P5C4		54.6 ± 11.2	0.080
P5C5		28.9 ± 1.9	0.080
P5C7		40.0 ± 4.7	0.071
P7C8		15.6 ± 5.1	0.085
P8C9		1.7 ± 0.3	0.101
P+		8.7 ± 4.2	0.057

Combination of the X-ray structures and IC₅₀ values suggest that the homocysteine-cyclised peptide, **P8C9**, retains the binding conformation of the peptide more effectively than the cysteine-cyclised peptide, likely due to the flexibility provided by the extra carbon atom on the amino acid side chain (ESI Fig S5). **P8C9** shows both an improved potency and an improved ligand efficiency compared to **P+** and, as such, represents a promising starting point for the development of potent and cell permeable CK2 PPI inhibitors.

The binding of **P8C9** to CK2α was further assessed using ITC (ESI Fig S6) and its K_d was found to be 750 nM. The serum stability of **P8C9** was also analysed; it was found that **P8C9** was fully stable in serum

over 24 h compared to the linear peptide **P8** which fully had degraded after 1 h (ESI, Fig S7). This was seen as a large improvement upon CAM7117 which is only 50% intact in serum after 24 h.¹⁶

X-ray crystallography

X-ray crystallography was used to confirm the binding mode of **P8C9**. Comparison of the co-crystal structures of **P8C9** and **P+** in complex with CK2 α indicates that the central binding sequence of the two peptides share the same binding conformation (Fig 2c).

Functionalisation of **P8C9** would be desirable for the incorporation of cell penetrating tags, fluorescent dyes etc; however, functionalisation through the staple is not facile due to the one-component stapling used. The crystal structure of **P8C9** suggests that functionalisation of the peptide may be possible through the *N*-terminus or the Lys residue as both are solvent exposed (Fig 2a and b). Indeed, functionalisation of the *N*-terminus of the peptide with a fatty acid and PEG chain only resulted in a minor decrease in binding affinity ($K_d = 750$ nM and 1.3 μ M for **P8C9** and **FA-P8C9** respectively ESI Fig S6), as did functionalisation of the Lys residue with a PEG chain⁵ ($K_d = 1.6$ μ M for **P8C9**[PEG], ESI Fig S6) indicating that the addition of large groups to either the *N*-terminus or the Lys residue of **P8C9** is likely to have little effect on its binding ability.

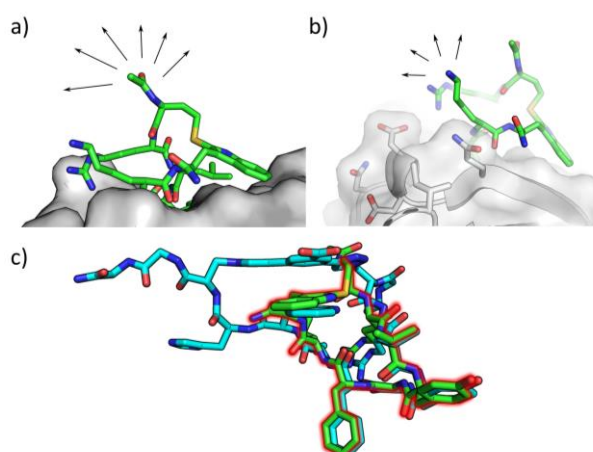


Figure 2. X-ray co-crystal structure of **P8C9** in complex with CK2 α (PDB: 6YZH). a and b) The *N*-terminus and Lys residue of **P8C9** are both solvent exposed making them good candidates as positions of functionalisation of the peptide. c) Overlay of the crystal structures of **P8C9** and **P+** in complex with CK2 α (PDB: 6Q4Q) highlighting that the central binding motif of the two peptides retain the same binding conformation.

Cell proliferation assay

Finally, the effect of **P8C9** was evaluated in HeLa cells to determine if the peptide was able to reduce cell viability. Unfortunately, **P8C9** had no effect on cell viability (ESI Fig S9). **FA-P8C9** was evaluated in cells and found to reduce the cell viability. However, **FA-PEG** alone was observed to cause some toxicity, and thus **FA-P8C9** was deemed to be causing partial non-specific toxicity (ESI Fig S10).

Nevertheless, functionalisation of the *N*-terminus of **P8C9** with the known cell penetrating peptide sequence TAT (GRKKRRQRRPPQ)²¹ joined to the peptide through a di-Ahx spacer, **TAT-P8C9**, resulted in a large reduction in cell viability (Fig 3), as did analogous functionalisation with a tri-Arg tag (**R3-P8C9**, Fig 3). No effect on cell viability was observed for the cell penetrating tag-spacer conjugates alone (**TAT-(Ahx)₂** and **R3-(Ahx)₂**, ESI Fig S12). Thus, both **TAT-P8C9** and **R3-P8C9** represent promising CK2 modulating peptides.

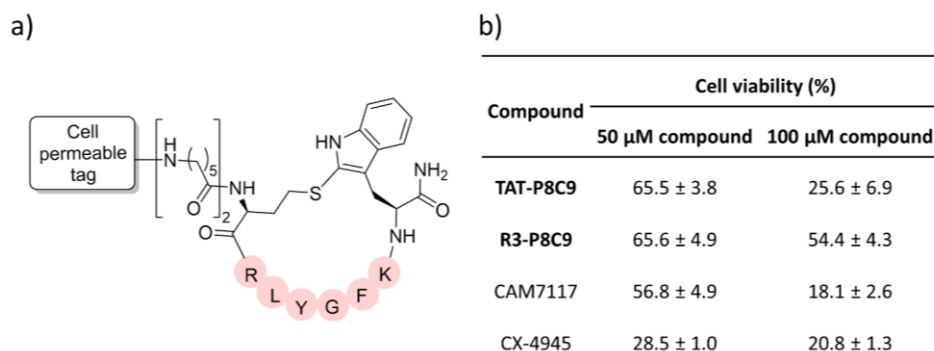


Figure 3. a) Structure of cell penetrating **P8C9** derivatives; CPP = TAT, **TAT-P8C9**; CPP = R3, **R3-P8C9**. b) Results of cell proliferation assay showing the percentage of viable cells remaining after treatment of HeLa cells with the specified compounds for 48 h. Average values are shown \pm standard deviation.

Conclusions

In conclusion, the structure of CAM7117 has been optimised to reduce its molecular weight whilst retaining good activity and its synthesis simplified. Various shortened cyclic peptides were synthesised and biologically evaluated. **P8C9** was found to exhibit similarly high potency to CAM7117 in enzymatic assays, as well as retaining the same binding conformation and displaying an increased stability compared to CAM7117. Functionalisation of **P8C9** is possible through two positions on the peptide and incorporation of the cell penetrating peptides TAT and tri-Arg onto the *N*-terminus of the peptide provided peptides with good cellular toxicity. **P8C9** is the smallest peptide CK2 binder to date displaying high serum stability. Its facile synthesis makes it a much more attractive chemical probe than CAM7117 and its small structure leaves room for optimisation of both efficacy and pharmacokinetic properties.

Conflicts of interest

There are no conflicts to declare.

Acknowledgements

This work was funded by the Wellcome Trust Strategic (090340/Z/09/Z) Award (to DRS and MH). In addition, the group research was supported by grants from the Engineering and Physical Sciences Research Council, Biotechnology and Biological Sciences Research Council, Medical Research Council and Royal Society. ELA would like to thank the Cambridge Trust and EPSRC for funding, JI would like to acknowledge the EPSRC and the Wellcome Trust for financial support. We would like to thank Diamond Light Source for access to and support at beamline iO4 (proposal 18548) and the Department of Biochemistry X-ray crystallographic and Biophysics facilities for access to instrumentation.

Notes

‡ Precipitation of **P5C6** occurred during the FP assay, most notably at the higher concentrations. The top concentration tested gave uninterpretable results (inhibition > 100%) and thus it has been removed from analysis. The error between the runs is significant and, as such, no IC_{50} is reported.

§ Precipitation of **P8C9[FA]** occurred during ITC testing and thus, no K_d value could be obtained for the Lys-functionalised fatty acid derivative of **P8C9**.

References

- 1) C. Borgo, C. D'Amore, L. Cesaro, S. Sarno, L. A. Pinna, M. Ruzzene and M. Salvi, *Crit. Rev. Biochem. Mol. Biol.*, 2021, **56**, 321–359.
- 2) J. Iegre, E. L. Atkinson, P. Brear, B. M. Cooper, M. Hyvönen and D. R. Spring, *Org. Biomol. Chem.*, 2021, **19**, 4380–4396.
- 3) A. Siddiqui-Jain, D. Drygin, N. Streiner, P. Chua, F. Pierre, S. E. O'brien, J. Bliesath, M. Omori, N. Huser, C. Ho, C. Proffitt, M. K. Schwaebe, D. M. Ryckman, W. G. Rice and K. Anderes, *Cancer Res.*, 2010, **70**, 10288–10298.
- 4) B. Guerra and O. G. Issinger, *Electrophoresis*, 1999, **20**, 391–408.
- 5) J. Hochscherf, D. Lindenblatt, M. Steinkrüger, E. Yoo, Ö. Ulucan, S. Herzig, O.-G. G. Issinger, V. Helms, C. Götz, I. Neundorff, K. Niefind and M. Pietsch, *Anal. Biochem.*, 2015, **468**, 4–14.
- 6) M. M. J. Chua, C. E. Ortega, A. Sheikh, M. Lee, H. Abdul-Rassoul, K. L. Hartshorn and I. Dominguez, *Pharmaceuticals*, 2017, **10**, 18.
- 7) J. H. Trembley, G. Wang, G. Unger, J. Slaton and K. Ahmed, *Cell. Mol. Life Sci.*, 2009, **66**, 1858–1867.
- 8) S. W. Strum, L. Gyenis and D. W. Litchfield, *Br. J. Cancer* 2021, 2021, 1–10.
- 9) P. Brear, A. North, J. Iegre, K. Hadje Georgiou, A. Lubin, L. Carro, W. Green, H. F. Sore, M. Hyvönen and D. R. Spring, *Bioorg. Med. Chem.*, 2018, **26**, 3016–3020.
- 10) K. A. Ahmad, G. Wang and K. Ahmed, *Mol Cancer Res*, 2006, **2**, 712–721.
- 11) M. Salvi, C. Borgo, L. A. Pinna, M. Ruzzene. *Cell Death Discov.* 2021, **7**, 325.
- 12) Search of: CX-4945 - List Results - ClinicalTrials.gov, <https://clinicaltrials.gov/ct2/results?cond=&term=CX-4945&cntry=&state=&city=&dist=>, (accessed 31 January 2022).
- 13) R. Prudent and C. Cochet, *Chem. Biol.*, 2009, **16**, 112–120.
- 14) P. Brear, C. De Fusco, K. Hadje Georgiou, N. J. Francis-Newton, C. J. Stubbs, H. F. Sore, A. R. Venkitaraman, C. Abell, D. R. Spring and M. Hyvönen, *Chem. Sci.*, 2016, **7**, 6839–6845.
- 15) J. Iegre, P. Brear, C. De Fusco, M. Yoshida, S. L. Mitchell, M. Rossmann, L. Carro, H. F. Sore, M. Hyvönen and D. R. Spring, *Chem. Sci.*, 2018, **9**, 3041–3049.
- 16) J. Iegre, P. Brear, D. J. Baker, Y. S. Tan, E. L. Atkinson, H. F. Sore, D. H. O' Donovan, C. S. Verma, M. Hyvönen and D. R. Spring, *Chem. Sci.*, 2019, **10**, 5056–5063.
- 17) L. Nevola and E. Giralt, *Chem. Commun.*, 2015, **51**, 3302–3315.
- 18) B. Laudet, C. Barette, V. Dulery, O. Renaudet, P. Dumy, A. Metz, R. Prudent, A. Deshiere, O. Dideberg, O. Filhol and C. Cochet, *Biochem. J.*, 2007, **408**, 363–373.
- 19) B. Bestgen, Z. Belaid-Choucair, T. Lomberget, M. Le Borgne, O. Filhol and C. Cochet, *Pharmaceuticals*, 2017, **10**, 16.
- 20) C. Puig Duran, F. Albericio Palomera, M. Gongora Benitez *et al.* WO/2019/030298, 2019-02–14.
- 21) A. D. Frankel and C. O. Pabo, *Cell*, 1988, **55**, 1189–1193.